

Numerical simulation of concrete beams reinforced with composite GFRP-Steel bars under three points bending

Ahmed S. Elamary^{*1,2} and Rafik K. Abd-ELwahab^{1a}

¹Faculty of Engineering, Department of Civil Engineer, Al-Azhar University, Qena, Egypt

²Department of Civil Engineering, Taif University, Taif, Saudi Arabia (Temporary)

(Received April 15, 2015, Revised January 26, 2016, Accepted January 29, 2016)

Abstract. Fiber reinforced polymer (FRP) applications in the structural engineering field include concrete-FRP composite systems, where FRP components are either attached to or embedded into concrete structures to improve their structural performance. This paper presents the results of an analytical study conducted using finite element model (FEM) to simulate the behavior of three-points load beam reinforced with GFRP and/or steel bars. To calibrate the FEM, a small-scale experimental program was carried out using six reinforced concrete beams with 200×200 mm cross section and 1000 mm length cast and tested under three point bending load. The six beams were divided into three groups, each group contained two beams. The first group was a reference beams which was cast without any reinforcement, the second group concrete beams was reinforced using GFRP, and the third group concrete beams was reinforced with steel bars. Nonlinear finite element simulations were executed using ANSYS software package. The difference between the theoretical and experimental results of beams vertical deflection and beams crack shapes were within acceptable degree of accuracy. Parametric study using the calibrated model was carried out to evaluate two parameters (1) effect of number and position of longitudinal main bars on beam behavior; (2) performance of concrete beam with composite longitudinal reinforcement steel and GFRP bars.

Keywords: GFRP bars; concrete beams; finite element model; composite reinforcement

1. Introduction

Reinforced concrete beams are commonly used in the majority of reinforced concrete structures, which might be subjected to water leakage and the application of deicing salts. The use of the corrosion free fiber-reinforced polymer (FRP) reinforcing bars in such structures is beneficial to overcome the steel-corrosion problems. FRP materials exhibit linear-elastic stress-strain characteristics up to failure, which raises concerns on their performance in beam subjected to vertical loads. Several codes and design guidelines (such as ACI-440-1R-2006, ACI-440-2R-2008, ISIS design manual No.3-2001 and CNR-DT 200/2004) are now available for the design of concrete structures reinforced with fiber-reinforced polymer (FRP) bars under flexural and shear loads.

*Corresponding author, Associated Professor, E-mail: a.elamary@tu.edu.sa, zshamary@gmail.com

^aLecturer, E-mail: dr.rkhaury@gmail.com

The objective of this study is to assess the flexural behavior of concrete beams reinforced with glass (G) FRP or composite GFRP and steel bars. Based on a small experimental programme a theoretical study of the load-deflection behavior of concrete beams reinforced with only steel or GFRP bars were conducted. Six reinforced concrete beams prototypes with 200×200 mm cross section and 1000 mm length cast and tested under three point bending. The six beams divided into three groups, each group contains two beams. The first group was a reference beams without any reinforcement, the second concrete beams reinforced longitudinally and confined with stirrups using GFRP, and the third group was concrete beams reinforced longitudinally and confined with stirrups with steel bars. Load vs. mid deflection curve and shape of cracks were compared to calibrate the finite element model. The comparison shows that, the model can simulate the actual behavior of concrete beams to an acceptable degree of accuracy. Using the finite element model created and verified, two main parameters related to the use of GFRP bars for strengthening reinforced concrete beams subject to three point bending were studied: (1) Effect of GFRP ratio on the behavior of concrete beams (2) the performance of concrete beam with composite longitudinal reinforcement steel and GFRP bars. Some of the previous work related to this study will be reviewed and summarized below:

(Thomas and Ramadass 2015) gave a model for the evaluation of shear strength of fiber reinforced polymer (FRP)-reinforced concrete beams. They tested eight beams reinforced with GFRP rebars without stirrups with shear span to depth ratio of 0.5 and 1.75. The concrete compressive strength was varied from 40.6 to 65.3 MPa. The longitudinal reinforcement ratio was varied from 1.16 to 1.75. The experimental shear strength and load-deflection response of the beams were determined and reported. A model was proposed for the prediction of shear strength of beams reinforced with FRP bars. The proposed model accounts for compressive strength of concrete, modulus of FRP rebar, longitudinal reinforcement ratio, shear span to depth ratio and size effect of beams. The shear strength of FRP reinforced concrete beams predicted using the proposed model was found to be in better agreement with the corresponding test data. (Panda *et al.* 2013) studied shear strengthening performance of simply supported reinforced concrete (RC) T-beams bonded by glass fibre reinforced polymer (GFRP) strips in different configuration, orientations and transverse steel reinforcement in different spacing. Eighteen RC T-beams of 2.5 m span were tested. Nine beams were used as control beam. The stirrups were provided in three different spacing such as without stirrups and with stirrups at a spacing of 200 mm and 300 mm. Another nine beams were used as strengthened beams. GFRP strips were bonded in shear zone in U-shape and side shape with two types of orientation of the strip at 45° and 90° to the longitudinal axis of the beam for each type of stirrup spacing. The experimental result indicated that, the beam strengthened with GFRP strips at 45° orientation to the longitudinal axis of the beam was much more effective than 90° orientation. Also as transverse steel increased, the effectiveness of the GFRP strips decreases. (Mini *et al.* 2014) reported the influence of number of layers and breadth of GFRP sheets wrapped onto RCC beams for strengthening. Twelve beams of size 700 mm×150 mm×150 mm were cast and tested. Two beams without GFRP and ten beams wrapped in different lay-up patterns with one and two layers of GFRP sheets was subjected to three point loading test and ultrasonic pulse velocity test. Initial crack load, ultimate failure load and types of failure have been observed and noted. Experimental results indicated a significant increase in initial and ultimate load carrying capacity of GFRP wrapped beams compared to unwrapped beams. GFRPs have been found attractive in Asia due to their cost competitiveness over carbon fiber composites (Saadatmanesh 1994, Karbhari 2001). Tests carried out on concrete beams reinforced externally with FRP plates indicate substantial increase in the strength of the

beams and decks (Wang *et al.* 2003, Arduini *et al.* 1997, Saadatmanesh *et al.* 1998, Malek *et al.* 1998, Teng *et al.* 2001). In recent years, the use of externally bonded FRP has become increasingly popular for civil infrastructure applications, including wrapping of concrete beams and columns. Significant research has been devoted to beams and columns retrofitted with FRP and numerous models were proposed. Some of these in the strengthening of steel structures, where carbon FRP is preferred to glass FRP due to its much higher elastic modulus and strength. The critical difference between FRP-to-concrete and FRP-to-steel bonded interfaces is that the concrete is usually the weak link in the former, while in the latter the adhesive is the weak link. Avoiding adhesive failure has been addressed in a separate study (Teng *et al.* 2010). Different test methods for bonded joints have been used by different researchers (Zhao and Zhang 2007). New approach that incorporates the effects of temperature, design life, and relative humidity (RH) of exposure into the environmental reduction factor (RF) for glass fiber reinforced polymer (GFRP) bars used as concrete reinforcement studied. By using time extrapolation and time-temperature shift approaches, a new equation for design strength of GFRP bar under various exposure time and temperature was proposed (Huang and Aboutaha 2010). Eight beams, including two control beams reinforced with only steel or only GFRP bars, were tested. The amount of reinforcement and the ratio of GFRP to steel were the main parameters investigated experimentally and theoretically. Hybrid GFRP/steel-reinforced concrete beams with normal effective reinforcement ratios exhibited good ductility, serviceability, and load carrying capacity. Comparisons between the experimental results and the predictions from theoretical analysis showed that the models they adopted could adequately predict the load carrying capacity, deflection, and crack width of hybrid GFRP/steel-reinforced concrete beams (Qu *et al.* 2009). The local bond mechanics of glass-fiber reinforced polymer (GFRP) bars in normal strength concrete was investigated through experimental testing and analytical modeling. The experimental program was comprised of 30 direct tension pullout specimens with short anchorages. Parameters considered were the bar roughness and diameter, the size effect expressed by the constant cover to bar diameter ratio, and the external confining pressure exerted over the anchorage length by transverse externally bonded FRP sheets. An analytical model of the bond stress-slip response of a GFRP bar was derived from first principles and calibrated against the test data of them investigation. Using the calibrated model, design values for bond and slip were estimated with reference to the code limit state model for bond (Tastani and Pantazopoulou 2006) This paper presents a comprehensive experimental study on the behavior of reinforced concrete beams under three points bending. These beams were reinforced using GFRP or/and steel bars. The main objective of this study is to find a new material that can be used as a partial replacement of the steel bars to minimize the cost and decrease the possibility of corrosion.

2. Experimental program

2.1 Test specimen details

In this study, six full-sized beams tested at the Research Building Centre in Giza, Egypt. The beams were tested under three points bending. The test specimen divided into three groups; each group contains two beams. The first group of beams was the reference beams without any reinforcement. The second group reinforced with GFRP bars with a square cross section of 10 mm and GFRP stirrups, where the third group reinforced using two steel bars 10 mm in diameter and

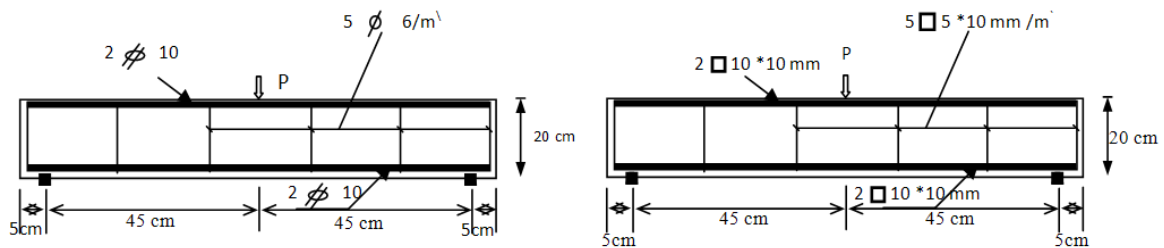
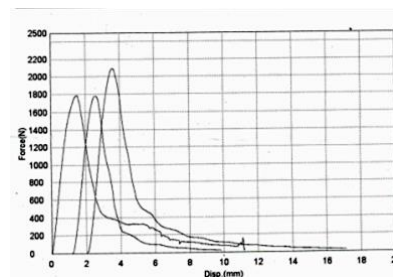


Fig. 1 Details of test specimens



(a) Test setup



(b) Test results

Fig. 2 Tensile test of GFRP bar specimens

steel stirrups. The length of each beam was 1000 mm and the cross section 200 mm \times 200 mm. The characteristic compressive strength of 28 days was 20 MPa and 25 MPa for plain concrete and reinforced concrete respectively. Yielding stress of longitudinal steel bars and stirrups was 360 MPa and 280 MPa respectively. After casting, all beams were cured at normal temperature in a water bath for 28 days. The plain concrete beams were called PC1/ PC2, while the beams reinforced by GFRP or steel were designated FRP1/FRP2 and RC1/RC2 respectively. The reinforcement details are shown in table1; where Fig. 1 shows the details of the test specimens.

2.2 Materials

The reinforcement materials used in the experimental program were from the commercially-available GFRP and steel bars. Ordinary locally-manufactured Portland cement having a specific gravity of 3.15 was employed in the casting of the specimens. Fine aggregate having a fineness modulus of 2.54 and a specific gravity of 2.62 was used. Coarse aggregate of 30 mm maximum size having a fineness modulus of 7.94 and specific gravity of 2.94 was used. The average standard 28-days compressive strength of concrete cubes was approximately 27 MPa with a mix weight ratio of cement: sand: gravel: water at 1:1.8:3.2:0.48. Tensile tests were conducted on three samples of GFRP having square cross section of 10 mm breadth to determine their ultimate tensile strength, ultimate strain and modulus of elasticity “180 MPa, 3.5% and 10500 N/mm² respectively”.

2.3 GFRP tensile test and test results

Three GFRP specimens were tested using tensile testing machine. The top end of the specimen

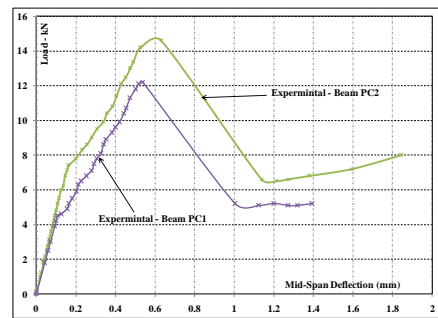
was fixed by grips on the top cross-head of the machine while the bottom end was pulled down. A load was applied at a constant speed until failure of the specimen. Fig. 2 shows the load displacement curve for the three specimens. All the failures started with splitting and ended with rupture of the bar.

3. Test results

The relationships between the total applied load and the measured mid-span deflection for the six tested beams are illustrated in Figs. 3(b),(d),(f). Through these figures it is observed that the presence of steel bars enhances the beams' deformability and hence ductility. Strut and tie mechanisms were employed in the beams reinforced with steel bars. The cracks at the failure stage



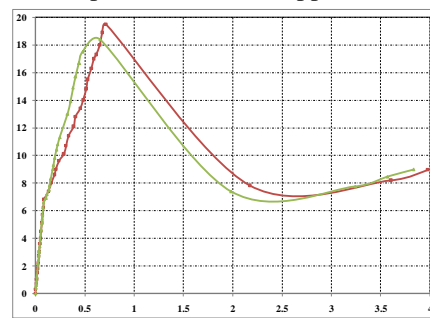
(a) Pattern of cracks shape of failure for beam (PC)



(b) Mid-span deflection vs. applied load, PC



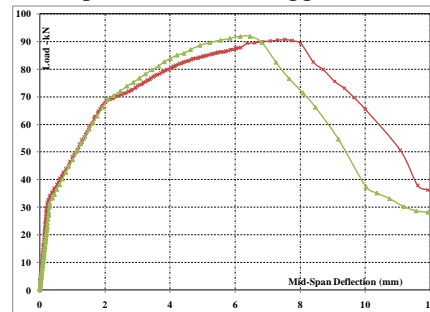
(c) Pattern of cracks, shape of failure for beam (FRP)



(d) Mid-span deflection vs. applied load, FRP



(e) Pattern of cracks, shape of failure of beam (RC)



(f) Mid-span deflection vs. applied load, RC

Fig. 3 Failure modes in PC, FRP and RC beams-crack patterns and failure shapes

in the GFRP-reinforced beam were mainly vertical cracks under the load line. These cracks had similar trajectory but were less width than the cracks in the plain concrete beams. In contrast, three cracks were formed in the RC beams, one vertical and two inclined, as shown in Fig. 3(e).

4. Finite element analysis

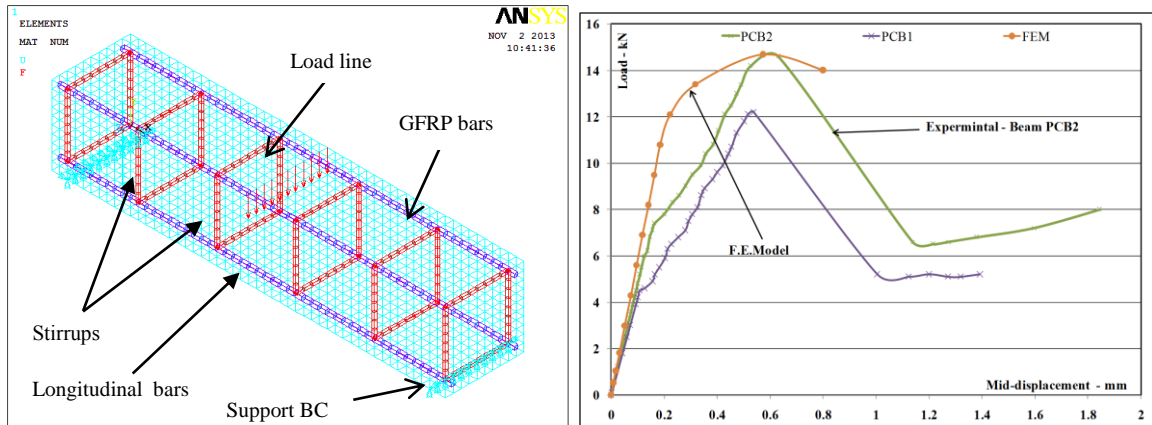
4.1 General

This study used finite element (FE) analysis by performing a numerical model representing full-sized tested beams. The boundary conditions of the FE model aimed to simulate the actual boundary conditions of the tested beams. Using load control techniques, central concentrated load applied at the top of the beam as a concentrated line load to simulate the load condition applied in the test as shown in Fig. 4(a). The out of plane displacement of the loaded points were restrained to prevent any lateral torsional effect. A three dimensional solid finite element model was constructed using the ANSYS finite element software. This program provides a dedicated three dimensional eight node solid isoparametric element, Solid65, to model the nonlinear response of brittle materials based on the constitutive model for the triaxial behavior of concrete (ANSYS Manual 2013).

The element includes a smeared crack analogy for cracking in tension zones and a plasticity algorithm to account for the possibility of concrete crushing in compression zones. Each element has eight integration points at which cracking and crushing checks are performed. The element behaves in a linear elastic manner until either of the specified tensile or compressive strengths is exceeded. Cracking or crushing of an element is initiated once one of the element's principal stresses, at an element's integration point, exceeds the tension or compressive strength of the concrete. Cracked or crushed regions, as opposed to discrete cracks, are then formed perpendicular to the relevant principal stress direction with stresses being redistributed locally. The amount of shear transfer across a crack can be varied between full shear transfer and no shear transfer (0.0) at a cracked section. The smeared stiffness and strut modeling options allow the elastic-plastic response of the reinforcement to be included in the simulation at the expense of the shear stiffness of the reinforcing bars. In this case the reinforcement modeled using strut elements is Link8. These elements are embedded in the mesh of Solid65 elements and the inherent assumption is that there is a perfect bond between the reinforcing bars and the surrounding concrete. A linear elastic perfectly plastic material law, described by the elastic modulus of the yield strength and post-yield stiffness of the material, was used for these elements. Dummy PIPE16 pipe elements were used to "line" the constraint equation region to provide the necessary rotational degrees of freedom at the nodes.

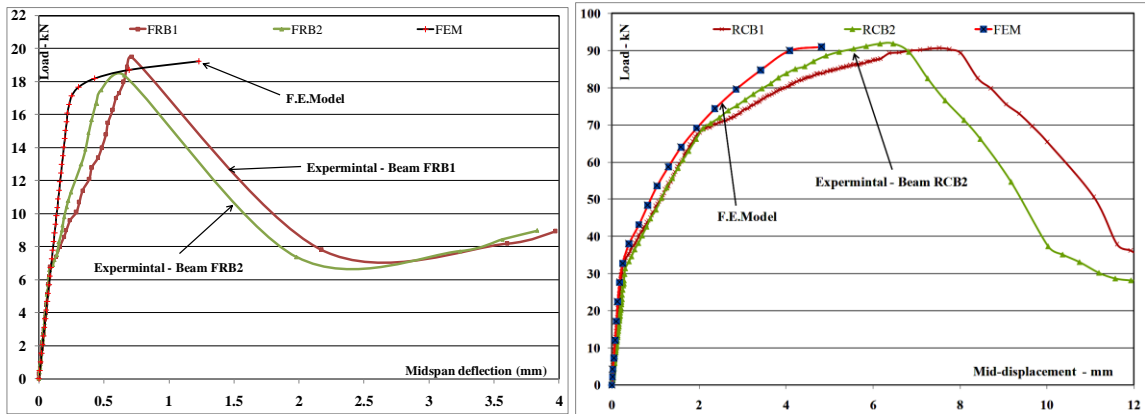
4.2 Model verification

Fig. 4(a) shows the FE models executed for the three beams to verify the performance of the model. Mid-span deflection versus applied load curves obtained from the FE models of PC2, FRP2, and RC2 are plotted in Figs. 4(b)-(c), and (d) respectively and compared with the experimental results. The comparisons shown in these figures confirm that the FE models can represent the beams to an acceptable degree of accuracy. Based on these models, parametric analyses were conducted to point out the effect of GFRP and/or steel bars on flexural behavior of



(a) Finite element model-Boundary conditions

(b) Experimental and FE model results-PC beams



(c) Experimental and FE model results-GFRP beams

(d) Experimental and FE model results-RC beams

Fig. 4 Comparison between experimental and FE model results

concrete beams. The analysis performed using force control techniques taken into consideration stress strain limitation and relationship for concrete, GFRP and steel bars materials. In all studied cases, the end of the analysis controlled by the crushing of the concrete elements and in minor cases the GFRP elements approach to ultimate tensile strength limit.

5. Parametric study

5.1 Introduction

In this parametric analysis two variables were studied: (1) the effect of GFRP bars number on the ultimate load concrete beam; and (2) the effect of hybrid steel-GFRP reinforcement on the behavior of concrete beam. It is possible to assess the effect of each variable graphically from Fig. 5 to Fig. 9.

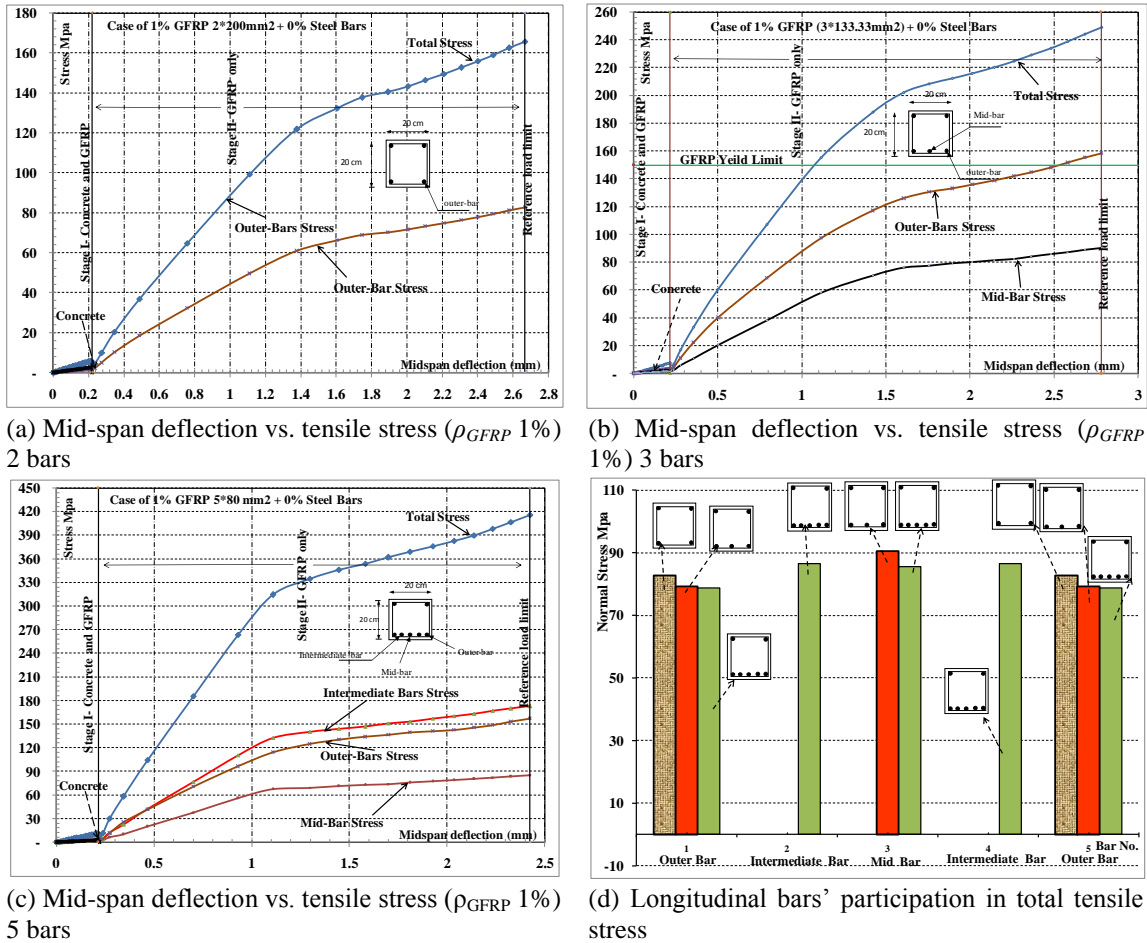
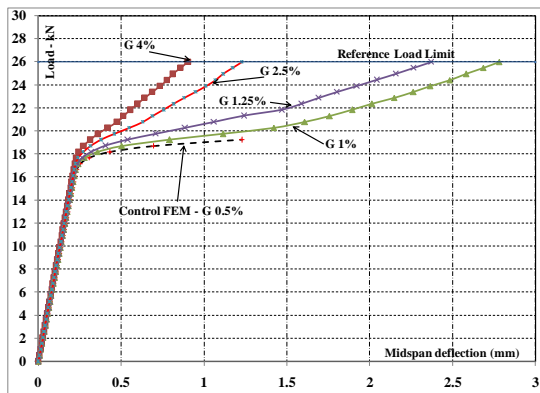


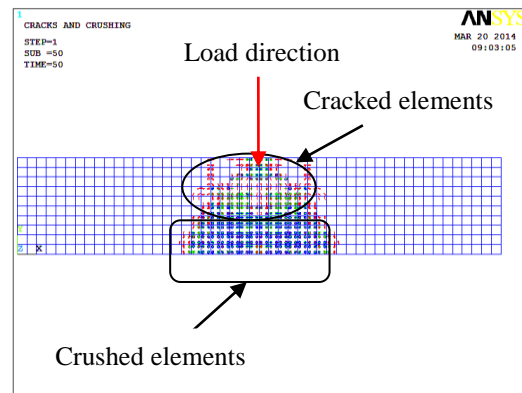
Fig. 5 Tensile stresses versus mid span deflection for different arrangements of longitudinal bars

5.2 Effect of number and position of longitudinal main bars

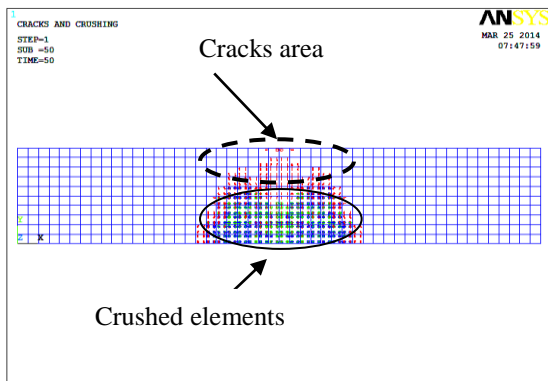
The effect of reinforcement bar configuration on the behavior of concrete beams can be examined by comparing the behavior of FE models results shown in Figs. 5(a),(b),(c). The previously analyzed beam with concrete compressive strength 25 MPa and $\rho_{GFRP}=1\%$ showed an ideal shape of strut and tie mechanism, thus it will be implemented as a reference for this part of study. The effect of numbers of longitudinal GFRP bars confined by GFRP rectangular stirrups studied in three different cases and the results obtained shown in this section. The total area of bars in each of these three cases was the same and equal to 400 mm^2 . Three different bar configurations studied in this section performed from n equal to 2, 3 and 5, where n is the total number of bottom reinforcement bars. The area of each bar in the three cases was 200 mm^2 , 133.33 mm^2 and 80 mm^2 respectively. The effect of number of longitudinal bars can be viewed in Figs. 5(a),(b),(c). These figures show the participation of concrete and each bar from overall stress applied and the total stress achieved in each case (165 MPa, 255 MPa and 400 MPa respectively). By increasing the number of longitudinal bars to five, the behavior of the beam changed significantly as shown in



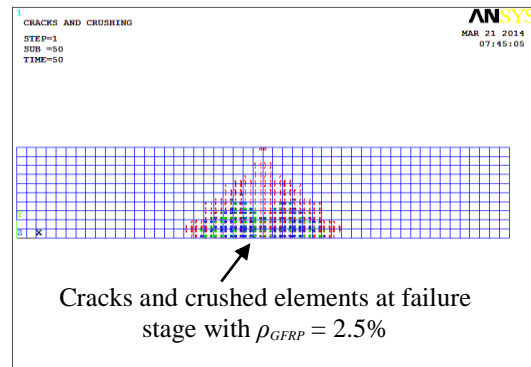
(a) Mid-span deflection vs. applied load-RC



(b) Pattern of cracks and crushed elements (ρ_{GFRP} 0.5%)



(c) Pattern of cracks and crushed elements (ρ_{GFRP} 1.25%)



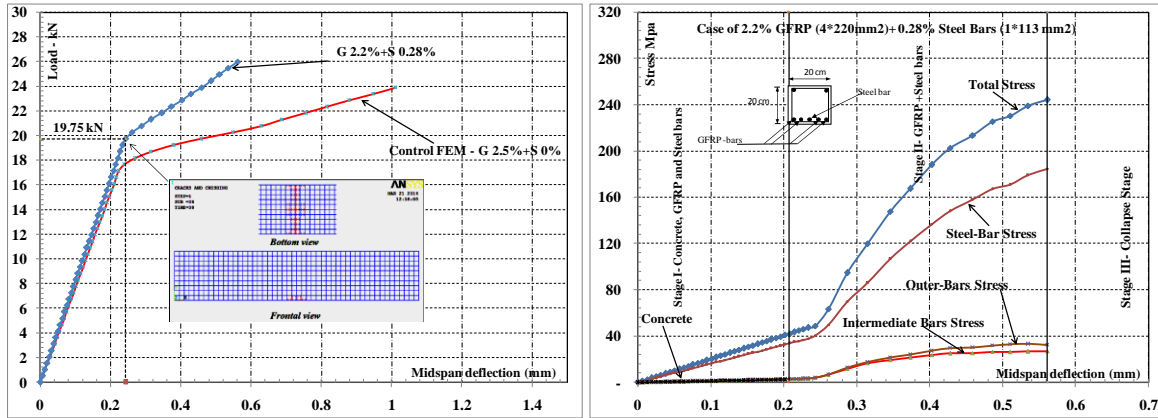
(d) Pattern of cracks-Strut and tie mechanism (ρ_{GFRP} 2.5%)

Fig. 6 Crack patterns and shapes of failure

Fig. 5(c). From these figures, it is seen that, the best performance of FRP2 beam represented by using five longitudinal bars. Finally, a comparison between the values of load carried out by each bar versus the bar number is plotted in Fig. 5(d). Here it can be concluded that the percentage of longitudinal bars is not the only factor that affects the performance of the beam, but also the positions of the bars has to be consider as an important factor.

5.3 Effect of composite steel and GFRP as longitudinal main bars

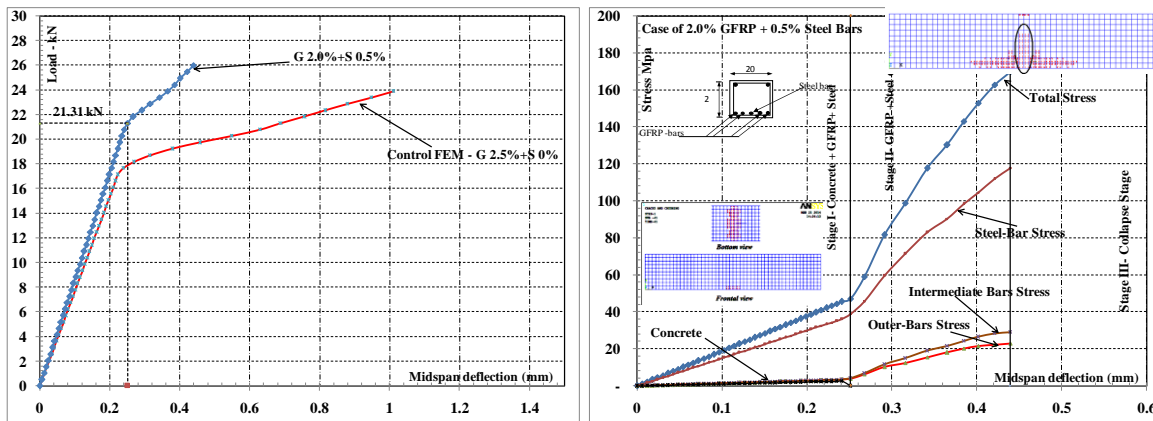
Fig. 6 shows the results of the analysis performed for concrete beams with five different ratios (0.5%, 1%, 1.25%, 2.5% and 4%) of GFRP area from beam cross section area. The purpose of this study is to point out the optimum GFRP ratio where ductile failure can be achieved and represented by strut and tie failure mechanism simulated at the end of the analysis by cracked and crushed elements. From this study it is concluded that, the ideal shape of failure mechanism achieved when GFRP bar area ratio was 2.5% and the ultimate load corresponding to failure stage was 26 kN. This result will be used as reference for studying the effect of hybrid reinforced steel and GFRP bars (with total ratio 2.5%) on the behavior of centrally loaded (26 kN) concrete beam.



(a) Mid-span deflection vs. applied load 90% GFRP 10% S

(b) Mid-span deflection vs. tensile stress

Fig. 7 Behavior and analysis of beam reinforced longitudinally using ρ_{GFRP} 2.2% and ρ_S 0.28%



(a) Mid-span deflection vs. applied load 80% GFRP 20% S

(b) Mid-span deflection vs. tensile stress

Fig. 8 Behavior and analysis of beams reinforced longitudinally using ρ_{GFRP} 2.0% and ρ_S 0.5%

This part of the parametric analysis studied the behavior of a concrete beam reinforced by composite steel and GFRP bars. The beam section was hybrid reinforced with composite steel and GFRP bars in longitudinal bottom bars with ρ_{GFRP} equal to 2.5% and longitudinal top bars of GFRP having the same area of the control FE model. Three different percentages of steel and GFRP bars were studied. The first beam had composite bottom reinforcement consisting of GFRP and steel. The ratios of GFRP and steel from 2.48% total beam reinforcement percentage were 2.2% and 0.28% respectively. In the second beam the portion of GFRP and steel was 2.0% and 0.5% with total reinforcement ratio 2.5%. For the third beam, the portions were $\rho_{GFRP}=1.73\%$ and $\rho_S=0.77\%$. From Fig. 7 to Fig. 9, it can be noticed that the concrete can carry a maximum 10% of the total tensile force produced by the bending moment action. Beyond that value, the zone subjected to tension is completely cracked and cannot sustain any further load. Now only the main bars are responsible for resisting the entire tension forces.

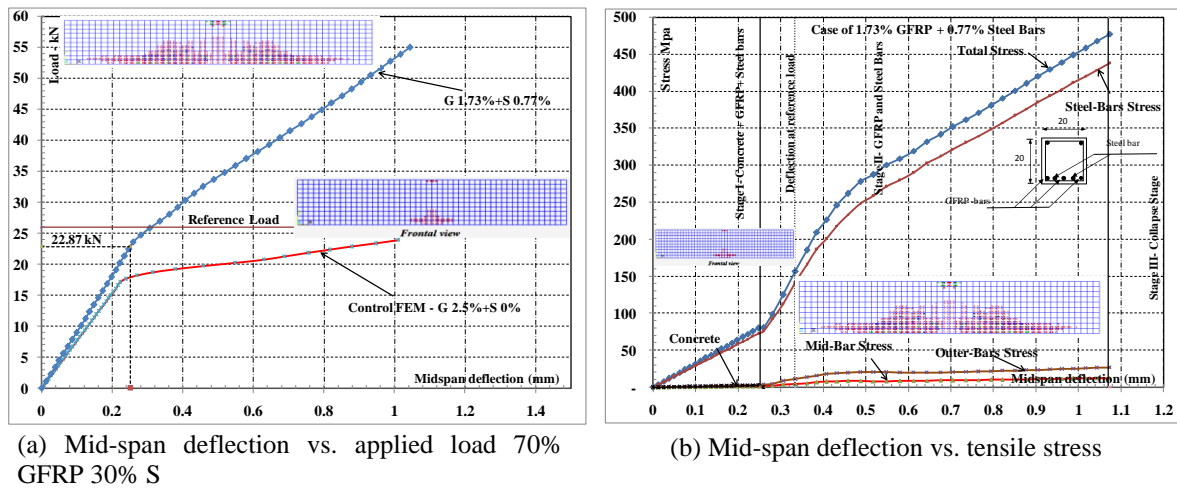


Fig. 9 Behavior and analysis of beams reinforced longitudinally using ρ_{GFRP} 1.73% and ρ_S 0.77%.

The contributions of each bar from the total tensile stress bred by the bending moment action are different and depend on the percentage of steel bars in each beam. Fig. 7 shows the percentage of participation of each bar from the total tensile stress for the first beam, with four bars of GFRP (2.2%) and one steel bar (0.28%). The percentage of the forced transferred by each bar is completely different in the second beam with four GFRP bars (2.0%) and one steel bar (0.5%) as illustrated in Fig. 8. The results also indicate that the area, position, and yield strength of longitudinal reinforcement have a significant effect on the ultimate capacity of the reinforced concrete beam.

From Fig. 7(a), it is seen that the load at the end of the elastic stage of beam behavior increased by 18%, and the number of crushed and cracked elements decreased significantly. Fig. 7(b) shows that, the tensile stress contribution of the steel bar was 75% of total applied tensile strength at a load equal to reference load, where each of the GFRP bars resisted 20 MPa.

In Fig. 8(a), the load at the end of elastic stage of beam behavior increased by 25%, and the number of crushed and cracked elements decreased significantly. From Fig. 8(b) it is concluded that, the tensile stress participation of the steel bar was 70% of total applied tensile strength at a load equal to the reference load, where each of the GFRP bars resisted 12 MPa.

Fig. 9(a) shows mid span deflection versus longitudinal tension for the third beam studied in this section. Characteristic concrete compressive strength was 25 MPa. It is noticed from this figure that, the steel bars can sustain all the applied tension force up to the reference load limit of 26 kN. The load at the end of the elastic stage of beam behavior increased by 37% and the number of crushed and cracked elements decreased significantly. From Fig. 9(b) it is concluded that, the tensile stress participation of the steel bar was 90% from total applied tensile strength at load equaling the reference load, where each GFRP bar resisted 12 MPa. To study the ability of the beam to sustain additional load and the participation of the GFRP bars in this load, the applied load was increased three times and the analysis of this beam continued to the collapse stage. Fig. 9 shows that the beam can sustain almost 55 kN. The GFRP started to participate in the resistance of the applied tension force after most outer elements of concrete were totally crushed. The maximum stress achieved by each bar of GFRP was 20 MPa from a total 470 MPa.

6. Conclusions

In this paper, an analytical investigation was conducted to evaluate the behavior of six 200 mm×200 mm×1000 mm concrete beams tested under central point loading. Two beams were reinforced using GFRP and two were reinforced with steel bars. Both types of reinforced beams were provided with rectangular stirrups made from the same material used in the longitudinal reinforcement bottom bars. The following conclusions were drawn:

- 1- The percentage of longitudinal bars was not the only factor that affects the performance of the beam; but also the positions and rearrangement of the bars were important factors.
- 2- In hybrid reinforced beams the area, position, and yield strength of longitudinal reinforcement were found to have a significant effect on the ultimate capacity of the reinforced concrete beam.
- 3- To ensure the participation of the GFRP bars in the flexural behavior of a concrete beam reinforced using hybrid steel and GFRP bars, the percentage of steel area may not exceed 20% of total reinforcement area. This percentage was verified experimentally and the results will be published in the second part of this research program.

References

- Arduini, M. and Nanni, A. (1997), "Parametric study of beams with externally bonded FRP reinforcement", *ACI Struct. J.*, **94**(5), 493-501.
- Huang, J. and Aboutaha, R. (2010), "Environmental reduction factors for GFRP bars used as concrete reinforcement: new scientific approach", *J. Compos. Constr.*, **14**(5), 479-486.
- Karbhari, V.M. (2001), "Material considerations in FRP rehabilitation of concrete structures", *J. Mater. Civil Eng.*, **13**(2), 90-7.
- Malek, A.M., Saadatmanesh, H. and Ehasani, M. (1998), "Prediction of failure load of R/C beams strengthened with FRP plate due to stress concentration at the plate end", *ACI Struct. J.*, **95**(1), 142-52.
- Mini, K.M., Alapatt, R.J., David, A.E., Radhakrishnan, A., Cyriac, M.M. and Ramakrishnan, R. (2014) "Experimental study on strengthening of R.C beam using glass fibre reinforced composite", *Struct. Eng. Mech.*, **50**(3), 275-286.
- Panda, K.C., Bhattacharyya, S.K. and Barai, S.V. (2013), "Shear strengthening effect by bonded GFRP strips and transverse steel on RC T-beams", *Struct. Eng. Mech.*, **47**(1), 75-98.
- Qu, W., Zhang, X. and Huang, H. (2009), "Flexural Behavior of Concrete Beams Reinforced with Hybrid (GFRP and Steel) Bars", *J. Compos. Constr.*, **13**(5), 350-359.
- Saadatmanesh, H. (1994), "Fiber composites for new and existing structures", *ACI Struct. J.*, **91**(3), 346-54.
- Saadatmanesh, H. and Malek, A.M. (1998), "Design guidelines for flexural strengthening of RC beams with FRP plates", *J. Compos. Constr.*, ASCE, **2**(4), 158-64.
- Tastani, S. and Pantazopoulou, S. (2006), "Bond of GFRP Bars in Concrete: Experimental Study and Analytical Interpretation", *J. Compos. Constr.*, **10**(5), 381-391.
- Teng, J.G., Caob, S.Y. and Lama, L. (2001), "Behaviour of GFRP-strengthened RC cantilever slabs", *Constr. Build. Mater.*, **15**(1), 339-49.
- Teng, J.G., Fernando, D., Yu, T. and Zhao, X.L. (2010), "Treatment of steel surfaces for effective adhesive bonding", *Proceedings of the 5th International Conference on FRP composites in Civil Engineering (CICE)*, China, Beijing.
- Thomas, J. and Ramadass, S. (2015), "Design for shear strength of concrete beams longitudinally reinforced with GFRP bars", *Struct. Eng. Mech.*, **53**(1), 41-55.
- Wang, Y.C. and Chen, C.H. (2003), "Analytical study on reinforced concrete beams strengthened for flexure and shear with composite plates", *J. Compos. Struct.*, **59**(1), 137-148.

Zhao, X.L. and Zhang, L. (2007), "State-of-the-art review on FRP strengthened steel structures", *Eng. Struct.*, **29**(8), 1808-23.

CC